Journal of Marine Systems 257 (2026) 104271

Contents lists available at ScienceDirect

Journal of Marine Systems

journal homepage: www.elsevier.com/locate/jmarsys

Primary production in relation to algal species composition in a warming Western Antarctic peninsula

Maria A. van Leeuwe [a,b,*], Alison L. Webb [a], Mareike G. Bach [a], Michael P. Meredith [c], Desiree den Os [d], Jacqueline Stefels [a]

[a] University of Groningen, GELIFES, PO Box 11103, 9700 CC Groningen, the Netherlands
[b] University of Groningen, Arctic Centre, PO Box 716, 9700 AS Groningen, the Netherlands
[c] British Antarctic Survey, High Cross, Madingley Rd, Cambridge CB3 0ET, UK
[d] Hanze University of Applied Sciences, PO Box 30030, 9700 RM Groningen, the Netherlands

ARTICLE INFO

Keywords:
Antarctica
Climate
Diatoms
Haptophytes
Phytoplankton
Primary production
Temperature

ABSTRACT

The Western Antarctic Peninsula is a key area in the Southern Ocean ecosystem. Dense microalgal communities not only support diverse wildlife, but can also exert a climatic influence through CO_2-uptake and the emission of climate-active gases like dimethylsulfide. The build-up of biomass is driven by high rates of primary production. In this paper, data are presented on primary production in Ryder Bay, a biologically-rich coastal area. Primary production was measured by means of ^{13}C-uptake, in spring and summertime between 2012 and 2022. Production rates were linked to algal community composition and oceanographic data collected at the site of the Rothera Time Series. To get more detailed information on species-specific production rates, specific algal growth rates were obtained from laboratory studies and historical data. In Ryder Bay, primary production rates were 0.025 ($\pm$ 0.024) mg C l^{-1} h^{-1} on average across all studies, and highest in February 2017. In spring, production was dominated by haptophyte algae with a low temperature optimum. Diatoms with higher growth rates and a higher temperature optimum thrive later in summer. For the near future, our data support the predictions that the warming of surface waters will stimulate algal growth rates, which will result in increased primary production. On longer timescales, ongoing ocean warming is expected to have strong negative effects on the occurrence of haptophytes like *Phaeocystis antarctica*. For polar diatoms, a temperature growth optimum may be passed. A potential shift in species composition is predicted, with ensuing consequences for primary production and biogeochemical cycles.

1. Introduction

The coastal zone of the Western Antarctic Peninsula (WAP) is one of the most productive areas in the Southern Ocean. In spring and summer, large algal blooms can develop in polynyas and sheltered bay areas (Arrigo et al., 2015; Mascioni et al., 2021) and along the shelf (Eveleth et al., 2017). Algal blooms may develop to more than 30 μg chlorophyll *a* l^{-1} (Van Leeuwe et al., 2020; Vernet et al., 2008). Part of the carbon that is sequestered by microalgae may be transferred to the higher trophic levels in the thriving Antarctic ecosystem, supporting charismatic megafauna like penguins, seals and whales (Clarke et al., 2007; Ducklow et al., 2012). Another part can be consumed and remineralized in the surface waters – within a so-called retention system (Smetacek et al., 1990) – part of the carbon eventually may be transported into the deep ocean (Boyd et al., 2024; Droste et al., 2025). Microalgae do not only consume CO_2, they also produce gases such as dimethylsulfide (Stefels et al., 2018; Webb et al., 2019) and halocarbons (Hughes et al., 2009), which are important in a climate forcing context.

In the WAP, algal growth is controlled by annual dynamics in environmental conditions including light, nutrients and temperature. In spring, the melting of sea ice and glacial ice results in a lower salinity of surface waters. Coinciding with increasing temperatures towards summer, this promotes the stabilization and stratification of surface waters, thus generating optimal light conditions for algal growth (Clarke et al., 2008; Eveleth et al., 2017; Vernet et al., 2008; Rozema et al., 2017). Nutrients are in ample supply, with micronutrients such as iron and

* Corresponding author at: University of Groningen, GELIFES, PO Box 11103, 9700 CC Groningen, the Netherlands.
E-mail addresses: m.a.van.leeuwe@rug.nl (M.A. van Leeuwe), a.l.webb@rug.nl (A.L. Webb), m.g.bach@rug.nl (M.G. Bach), mmm@bas.ac.uk (M.P. Meredith), d.den.os@pl.hanze.nl (D. den Os), j.stefels@rug.nl (J. Stefels).

https://doi.org/10.1016/j.jmarsys.2026.104271
Received 25 November 2025; Received in revised form 14 July 2026; Accepted 21 July 2026
Available online 25 July 2026

manganese released from the shelf sediments and the multitude of nearby glaciers (Arrigo et al., 2015; Bown et al., 2018) and macronutrients supplied to the coast by upwelling of nutrient-rich Upper Circumpolar Deep Water (Henley et al., 2017, 2019; van Leeuwe et al., 2022). Seasonal warming further stimulates primary production in the course of summer, with a direct coupling between algal growth rates and temperature (Davison, 1991; Eppley, 1972; Edwards et al., 2016).

There remains limited insight in the impact of global warming on algal production in the WAP. During the second half of the 20th century, environmental conditions have changed rapidly. Temperatures in the surface waters of the WAP rose climatically by more than 1 °C (Clarke et al., 2007; Meredith and King, 2005). In addition, summer heatwaves are a new phenomenon, with locally seawater surface temperatures rising by almost 2 °C within a months' time (Latorre et al., 2023). Ocean warming has resulted in concurrent decreases in sea ice extent over a wide area of the Bellingshausen Sea and surroundings since at least the start of the satellite era in the 1970s (Eayrs et al., 2021; Stammerjohn et al., 2003, 2008). These sea ice changes consisted of a significant trend towards later advance in autumn, and a more moderate trend towards earlier retreat in spring. More recently, sea ice extent around Antarctica has shown dramatic extremes, with successive record highs in circumpolar sea ice extent during 2012–2014 followed by several years of record lows, including 2022–2023 (Reid et al., 2020; Stammerjohn et al., 2025). At the WAP, a marked retreat of sea ice was observed in summer 2016 concurrent with an unprecedented circumpolar retreat of sea ice.

Sea-ice dynamics strongly influence the stability of the water column, together with glacial melt and wind conditions (Deppeler and Davidson, 2017; Höfer et al., 2019; Schofield et al., 2024). In years with limited sea-ice extent, so-called "low-ice years", the water column is deeply mixed in spring. Following these years, stratification of surface waters occurs relatively late in the season (Schofield et al., 2024; Venables et al., 2013). At the same time, the warming of the WAP area has resulted in the acceleration of glacial melt (Schofield et al., 2024), enhancing water column stability. Changes in stratification have become apparent especially in the northern part of the WAP. Increased input of fresh meltwater into the coastal areas has resulted in the strengthening of stratification of surface waters later in the season, despite increasing storminess recorded since the 1980s (Schofield et al., 2024). As a net result, a delayed but overall extended growth season was observed, with a subsequent increase in primary production in the north over the last decades (Ferreira et al., 2024; Moreau et al., 2015; Prakash et al., 2025; Smith and Comiso, 2008). The increase in production was coupled to changes in algal species composition, with a decrease in the abundance of large diatoms versus an increase in cryptophyte species (Antoni et al., 2024; Mendes et al., 2023; Moline et al., 2004; Montes-Hugo et al., 2009). Up to present, these changes are less apparent further south along the Peninsula.

In order to better predict how primary production will develop in the future, it is necessary to know how the various algal groups contribute to primary production, and how these groups will respond to climate change. Previously, a seasonal shift in the composition of the algal community was observed in Ryder Bay (Van Leeuwe et al., 2020). The purpose of the current study is therefore twofold. Firstly, to further examine the link between primary production and the phenology of algal species in Ryder Bay, thereby incorporating the role of sea ice as a driver of these seasonal dynamics. Secondly, to investigate how the community might respond to climatically warming waters. It is known that algal species can adapt to temperature changes, but within limits. In general, Antarctic phytoplankton are adapted to the low ambient temperatures in polar waters, with growth optima that roughly range between 2 and 5 °C (Coello-Camba and Agustí, 2017). Species-specific response to ocean warming can be expected, based on differences in temperature tolerances. Only few extensive time series are available on primary production in the WAP (Goldman et al., 2015; Rozema et al., 2017). This study will present new data on primary production in Ryder Bay and assess the relationship between algal growth rates and temperature.

As a part of the wider Marguerite Bay area, Ryder Bay makes an excellent study site. Biological oceanography has been studied for more than three decades through the "Rothera Time-Series" (RaTS; Annett et al., 2010; Rozema et al., 2017; Van Leeuwe et al., 2020; Venables et al., 2023). To gain information on algal production rates, primary production was studied by means of ^{13}C-incorporation assays from November to March, between 2012 and 2022. Production data were linked to algal species composition and oceanographic data, to acquire further insight in causal influences and ecosystem functioning. The present paper follows from related works in Ryder Bay that have investigated climatic forcing and marine feedbacks in this area (Stefels et al., 2018; Van Leeuwe et al., 2020; Webb et al., 2019). Data from laboratory and literature studies were added to reveal potential differences in growth rates that might shed further light on the dominance of the particular algal groups observed in Ryder Bay. The consequences of a warming WAP on the functioning of the marine ecosystem are discussed.

2. Materials and methods

2.1. Field sampling

Seawater samples were taken from the RaTS site at 67.570°S, 68.225°W in Ryder Bay (Fig. 1). Five seasonal studies were conducted over the course of nearly ten years. Ryder Bay was studied extensively in 4 years, between November 2012 and March 2017. The bay was revisited in November–December 2022. Seawater samples were taken preferably twice a week, with a total of 87 sampling events. Discrete samples were collected from the water column at 15 m depth with Niskin bottles deployed using a hand winch from a small rigid inflatable boat. Full profiles were sampled at 5, 15, 25 and 40 m depth in 2014 and 2015–2016. In addition, in 2022 microphytobenthic samples were collected by divers. In 2022, benthic samples were taken using a 50 ml syringe (non-quantitatively) from 4 shallow sites in the vicinity of Rothera Research Station (Fig. 1). The pelagic and benthic samples were stored in the dark until further treatment in the laboratory, where

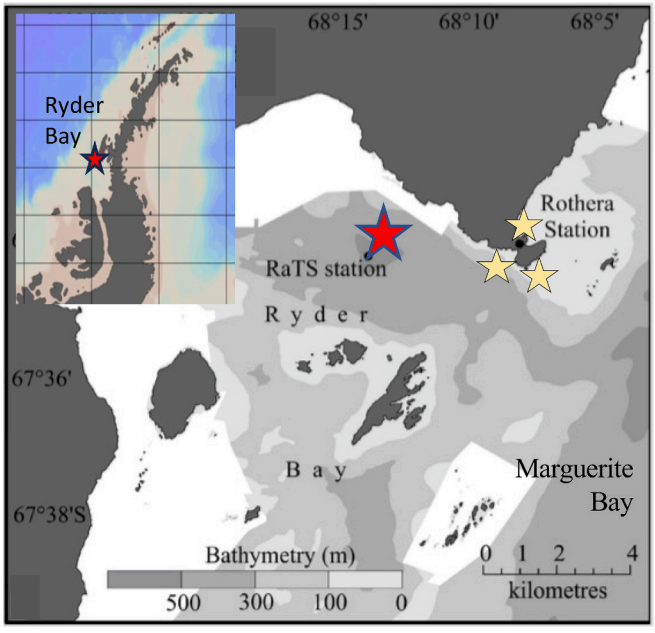

Fig. 1. The RaTS sampling station on Adelaide Island in Ryder Bay (red star), located at the Western Antarctic Peninsula (insert). Yellow stars indicate the locations of benthic sampling. (For interpretation of the references to colour in this figure legend, the reader is referred to the web version of this article.)

subsamples were taken for ^{13}C-incubations and ancillary parameters.

Alongside the seawater sampling, a Seabird 19+ conductivity, temperature and depth (CTD) instrument was deployed, combined with a WetLabs in-line fluorometer and LiCOR photosynthetically active radiation (PAR) sensor. Sea-ice cover in the bay was assessed visually on a daily basis by observers on the station: 100% sea ice cover was characterised by zero visible open water, and 0 % was no visible ice. For further details on oceanographic data collection and sea-ice cover in Ryder Bay, see https://www.bas.ac.uk/ project/rats/.

2.2. Primary production

2.2.1. ^{13}C-uptake experiments

Primary production was determined by means of ^{13}C-carbon incorporation into particulate organic carbon (POC). Assays were performed with samples collected from 15 m depth in 23 experiments (Table S1). Photosynthesis-irradiance (P-I) relationships were established by incubations of duplicate seawater samples at 6 light intensities, ranging from 5 to 500 μmol photons m^{-2} s^{-1}. In seasons 2012–2013, 2013–2014 and 2022–2023, experiments were performed indoors under controlled conditions of light and temperature, with approximately 10 h of light exposure at 2 °C. In seasons 2015–2016 and 2016–2017, an outdoor incubator was used. A similar range of light intensities was established as applied indoors, using neutral density filters. Temperature in the outdoor container was maintained at approximately 2 °C using continuous seawater flow-through. In addition, primary production was measured in samples collected at 5, 15, 25 and 40 m in the summer of 2013–2014 and 2015–2016 (Table S1). These samples were not subjected to a range of light intensities, but incubated indoors, at a fixed light intensity of 70 μmol photons m^{-2} s^{-1}, for circa 10 h.

Before incubation, a volume of 8–10 liter of collected seawater was enriched with a 590 mM $NaH^{13}CO_3$ stock solution to give a 5–8% final solution. This volume was distributed over 1500 ml gastight PFA bags (based on perfluoralkoxy, Ingeniven), for incubation. In 2022, microphytobenthic samples (non-quantitively) were placed in a 1 liter glass serum bottle with filtered seawater, which was then distributed over 250 ml TPP tissue culture flasks (Techno Plastic Products) for incubation. To determine the exact amount of $NaH^{13}CO_3$ added, 20 ml subsamples for dissolved inorganic carbon (DIC) were immediately taken from the bulk to which the $NaH^{13}CO_3$ was added. These t_0 samples were fixed with 10 μl saturated $HgCl_2$ and stored at 4 °C for later analysis. Incubations were then started by light exposure, and terminated by vacuum filtering the samples over 2.5 cm pre-combusted GF/F filters (Whatman, UK) at low vacuum (<15 kPa). Filters were snap-frozen in liquid nitrogen and stored at −20 °C prior to later analysis at the home laboratory.

2.2.2. Carbon analyses

DIC samples from t_0 were analysed by adding a 0.5 ml subsample to 10% orthophosphoric acid (H_3PO_4). The emerging CO_2 was purged with ultra-pure N_2 and analysed with a Cavity Ring-Down Spectroscopy analyser (CM-CRDS, with a G2101-i Analyser, Picarro, California, USA) that discriminates between the isotopes ^{12}C and ^{13}C. POC samples were acid-treated before analyses to remove inorganic carbon. The filters were left in a desiccator with 4 ml 37% fuming HCl for 4 h and dried at 60 °C. Filters were then packed in tin cups, which were placed in a combustion module attached to the Cavity Ring-Down Spectroscopy analyser. Specific carbon-incorporation rates (μ_{POC} (h^{-1})) were derived from the equation for production of DMSP in Stefels et al. (2009):

$$\mu_{POC}\left(h^{-1}\right) = \ln\left[\left(\left(R_m - R_b\right)/\left(R_m - R_t\right)\right)/\partial t\right] \quad (1)$$

in which R_m is the percentage of ^{13}C in dissolved inorganic carbon in the medium after addition of labelled $NaH^{13}CO_3$; R_b is the background percentage of $^{13}C/^{12}C$ in POC at t_0, and R_t is the percentage of ^{13}C in POC after incubation. Rate values obtained in the P-I experiments were taken to calculate the maximum growth capacity (P_{max}), light affinity α (mg C (mg Chl *a*)$^{-1}$ h^{-1} (μmol photons m^{-2} s^{-1})$^{-1}$) and the light saturation parameter E_k (μmol photons^{-1} m^{-2} s^{-1}), using a non-linear fit based on the photosynthesis-irradiance equation by Platt et al. (1980). The maximum growth capacity (P_{max}) was expressed in three ways. Firstly, as specific growth rate P^{μ}_{max} (h^{-1}). Secondly, as maximum primary production rate, P^{C}_{max} (mg C l^{-1} h^{-1}) that was obtained by multiplying P^{μ}_{max} with the carbon concentrations of the incubated samples. P^{C}_{max} was then normalized to chlorophyll *a* to calculate P^{Chl}_{max} (mg C (mg Chl *a*)$^{-1}$ h^{-1}).

The production rates that were obtained at the fixed light intensity of 70 μmol photons m^{-2} s^{-1} ($P_{70\mu E}$) were likewise expressed in three ways, as $P_{70\mu E}{}^{\mu}$, $P^{C}_{70\mu E}$ and $P^{Chl}_{70\mu E}$. $P^{C}_{70\mu E}$ recorded between 5 and 40 m was used to calculated the integrated production ($\sum PP$) over the water column:

$$\sum PP\left(g\,C\,m^{-2}d^{-1}\right) = \sum_{0}^{40}\left[\left(P^{C}_{70\mu E\_d1} + P^{C}_{70\mu E\_d2}\right)\Big/2\times\left(d_2 - d_1\right)\right] \quad (2)$$

in which d_1 is the shallower and d_2 the deeper depth (m). The top surface layer was integrated over 0–15 m, based on the average production at 5 and 15 m.

2.3. Ancillary parameters

2.3.1. Algal pigments

A sample volume of 1000–5000 ml seawater was filtered gently (< 15 kPa) over Whatman GF/F filters under dim light conditions, subsequently snap-frozen in liquid nitrogen, and stored at −80 °C until analysis at the home laboratory. Before extraction in 90% acetone, filters were freeze-dried at −55 °C for 48 h. Pigments were analysed by high-performance liquid chromatography (HPLC) on a Waters system. For full details on methods and pigment data, see Van Leeuwe et al. (2020). From the HPLC-dataset, chlorophyll *a* (Chl *a*) was retrieved as a measure of algal biomass. In addition, chlorophyll *a* was derived from fluorescence data collected by the CTD, to establish an extended time series over 2022–2023. Besides Chl *a*, the HPLC-dataset was used to determine algal groups based on algal marker pigments, from 2012 to 2017 (Van Leeuwe et al., 2020). Chemtax was set-up to distinguish between prasinophytes, cryptophytes, chlorophytes, diatoms and haptophytes. The data presented in the current manuscript have been extracted from the former paper. Only the major groups (cryptophytes, diatoms and haptophytes) will be addressed.

2.3.2. PAM fluorescence

The maximum quantum yield of fluorescence (F_v/F_m) as a measure of photosynthetic performance was determined using a pulse-amplitude-modulated (PAM) fluorometer (Water PAM, Heinz Walz, GmbH). Prior to each analysis, samples were dark-acclimated at 4 °C for 10–20 min. For each sample, the gain-settings of the fluorometer were tuned to the ambient algal concentrations, for optimal accuracy of the fluorometer.

2.3.3. Microscopy

Between 2012 and 2017, the composition of the algal community has been studied in close detail. Cell samples were preserved in an adapted Lugol's solution (based on iodine and glutaraldehyde; 0.5% final concentration) and analysed at home with an inverted microscope (Olympus IMT-2). Further details have been published in Van Leeuwe et al. (2020). In 2022, the samples that were collected for a qualitative analysis of the algal composition were examined within hours of collection by light microscopy (Zeiss).

2.4. Laboratory culture experiments

Between 2015 and 2025, growth experiments were performed with two diatom species, *Fragilariopsis cylindrus* (CCMP 1102; $n = 14$) and *Chaetoceros brevis* (CCMP 163; $n = 10$) and two haptophytes, *Phaeocystis antarctica* (CCMP 1871; $n = 20$) and *Chrysochromulina* sp. (CCMP 1215;

$n = 6$). The microalgae were cultured in batch monocultures, at 2–4 °C under a 16: 8 h light: dark regime. Cultures were grown in 250–500 ml glass bottles under nutrient- and light saturated conditions, with irradiance varying between 20 and 100 μmol photons m^{-1} s^{-1}. Cultures were kept in suspension by daily shaking. Specific growth rates were determined during the exponential phase of the growth curve through two methods. Firstly, ^{13}C-incorporation experiments were performed using the same methodology as described above, following formula 1 (Section 2.2). Secondly, cell counts were determined using light microscopy (Olympus CX41RF), counting a minimum of three replicate samples at two times during the exponential growth phase. Specific algal growth rates were calculated as.

$$\mu\ (d^{-1}) = [(\ln(N_t) - \ln(N_{t0}))/(t - t_0)] \quad (3)$$

where t is the period of time after the start (t_0) of the experiment and N is the number of cells.

The growth rates that were determined in the laboratory of the University of Groningen (RUG) were compared with values from a comprehensive literature search for similar Antarctic species. Some studies involved multiple environmental conditions (see Table S2). For this overview, specific growth rates were taken that were closest to natural conditions.

2.5. Statistical analyses

The biomass-related parameters POC and Chl *a* were tested with a two-way ANOVA, followed by a Tukey-test, with month and year of study as factors. The POC/Chl a ratio was tested with a mixed-effects analyses. The dataset of the other growth variables was too small for an ANOVA-test on month and year as factors. These variables were averaged over the year (Table 1), and differences tested with a *t*-test. The relationship between algal production (P^{μ}_{max} and P^{C}_{max}) and biological and oceanographic parameters measured over all study years was tested with a Spearman Rank Correlation analysis. Differences in species-specific growth rates (Table 3) were examined by *t*-tests. All test were performed using Graphpad Prism, applying a significance level of $p < 0.05$.

3. Results

3.1. Oceanography and primary production in Ryder Bay

In Ryder Bay, sea-ice cover varied across the years of sampling (Fig. 2). Whereas annual variations were coupled to large scale sea-ice dynamics along the WAP, variations within each year were influenced by sea-ice drifting in and out of the bay. In early November 2012, Ryder Bay was completely covered by sea ice, followed by a rapid decline towards December (Fig. 2). November 2013 had very little ice, except from a brief period of increased sea-ice cover in December. Whereas in 2015 moderate ice cover was observed throughout spring and summer, Ryder Bay remained fully ice-covered until December 2016, followed by a rapid decline of sea-ice in early January 2017. In 2022, sea ice was absent (no data plotted).

In early November of all years, the seawater temperature recorded at 15 m depth, averaged around −1.6 °C. The temperature increased gradually over the season, at variable pace (Fig. 2). In 2012–2013, temperatures rapidly increased in December, with high temperatures of more than 1.5 °C recorded in December and January. In contrast, subzero surface temperatures were recorded almost throughout the whole season in 2015–2016. In 2016–2017, seawater increased above 0 °C only in late January 2017. In 2022, temperatures started to increase end of November, reaching values of nearly 1 °C in February 2023 (Fig. 2).

In Ryder Bay, the algal growth season starts in November. When the various studies are compared, 2016–2017 significantly stands out as a high biomass study year (Fig. 3; two-way ANOVA, Tukey). When this year was taken out, a significant seasonal effect was observed (Two-way ANOVA). In 2013–2014, significant increases in POC and Chl *a* were observed from early December onwards, whereas biomass increased only by the end of December, early January in 2015–2016 and 2016–2017 (Fig. 3). High concentrations for POC and Chl *a* were recorded in February and March 2017 (Fig. 3, Table 1), with a maximum value of 4.9 mg C l^{-1} in February (Fig. 3). In contrast, the ratio of POC/Chl *a* declined from November onwards in 2013–2014 and from December onwards in 2015–2016 (Fig. 3; mixed-effect analysis).

There was no significant difference between the seasons, for the growth parameters P^{μ}_{max}, P^{C}_{max} and P^{Chl}_{max}, even though a high value for P^{C}_{max} almost up to 0.1 mg C l^{-1} h^{-1} was observed in February (CI 0.008–0.080), with elevated values in March 2017 (Fig. 3). Only in 2012–2013 and 2022, P^{Chl}_{max} was significantly higher compared to the other years (Table 1, *t*-test). In addition, light affinity (α) was highest in 2022 (Table 1, t-test). In contrast, Fv/Fm was significantly lower in 2012–2013. The light saturation parameter (E_k) was without any significant differences between the studies. Within each study season, the parameters did not show a significant temporal trend (Fig. 3). Only in 2022, P^{Chl}_{max} increased during November and December (Fig. 3, t-test).

In early spring 2013–2014 and 2015–2016, haptophytes were the most abundant algal group (Fig. 3). Diatoms dominated from December to January onwards (Fig. 3). Sporadic blooms of cryptophytes were observed later in summer 2012–2013 and 2013–2014 (Fig. 3). In November and December 2022, a mixture of algal species occurred. Besides unidentified flagellates, a variety of diatom species, including many small *Thalassiosira* and *Chaetoceros* species were observed (Table S3).

Spearman Rank correlation revealed a significant positive relationship between P^{C}_{max} and communities dominated by diatoms, which occurred later in the season, at zero-plus seawater temperatures (Fig. 5, season, Temp). P^{μ}_{max} showed similar relationships, but with lower correlation values. The late summer months were also positively related

Table 1
Growth variables (average ± sd) for seawater samples taken at 15 m depth in Ryder Bay, during the study years between 2012 and 2022. In addition, P^{μ}_{max} and Fv/fm were determined for benthos sampled in 2022 only.

	2012–2013	2013–2014	2015–2016	2016–2017	2022
P^{μ}_{max}	0.036 ± 0.004	0.048 ± 0.012	0.026 ± 0.022	0.039 ± 0.014	0.032 ± 0.005
P^{C}_{max}	0.016 ± 0.009	0.014 ± 0.008	0.011 ± 0.011	0.052 ± 0.030	0.015 ± 0.011
P^{Chl}_{max}	6.6 ± 4.2 [a]	1.6 ± 0.7	2.7 ± 1.6	2.7 ± 1.2	8.2 ± 2.7 [a]
α	0.04 ± 0.02	0.02 ± 0.01	0.03 ± 0.01	0.04 ± 0.01	0.07 ± 0.02 [a]
E_k	236 ± 175	96 ± 27	65 ± 56	86 ± 52	123 ± 58
Fv/Fm	0.58 ± 0.04 [a]	0.66 ± 0.07	0.65 ± 0.02	0.63 ± 0.06	0.70 ± 0.07
P^{μ}_{max} - benthos *	n.d.	n.d.	n.d.	n.d.	0.018 ± 0.004
Fv/Fm – benthos	n.d.	n.d.	n.d.	n.d.	0.62 ± 0.07

Units of the consecutive variables: P^{μ}_{max}: (h^{-1}); P^{C}_{max} (mg C l^{-1} h^{-1}); P^{Chl}_{max} (mg C (mg Chl *a*)$^{-1}$ h^{-1}); α (mg C (mg Chl *a*)$^{-1}$ h^{-1} (μmol photons m^{-2} s^{-1})$^{-1}$); E_k (μmol photons m^{-2} s^{-1}). [a] Significantly different from other years (*t*-test). For all data, see DOI: https://dataverse.nl/privateurl.xhtml?token=607fd7e1-77c8-4b48-9772-e669068dd9ad

* Since benthos did not show any sign of photoinhibition, production rates at 300 μmol photons m^{-2} s^{-1} were taken as P_{max}.

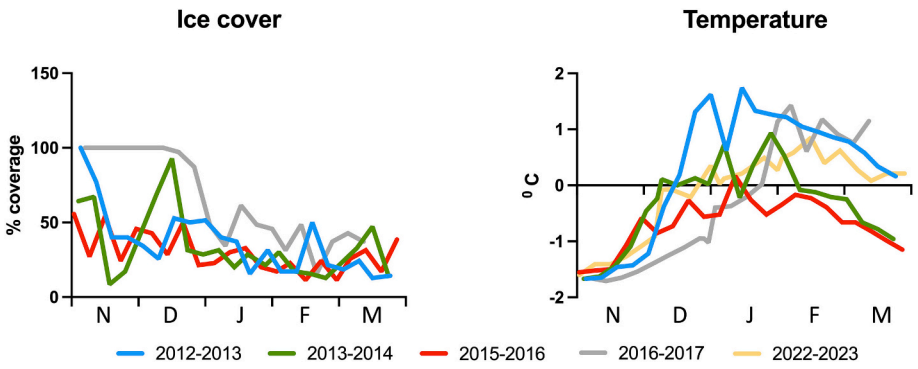

Fig. 2. Seasonal development of ice cover (%) and seawater temperature (°C; 15 m depth) at Ryder Bay (weekly averages), from November (N) till March (M), between 2012 and 2023.

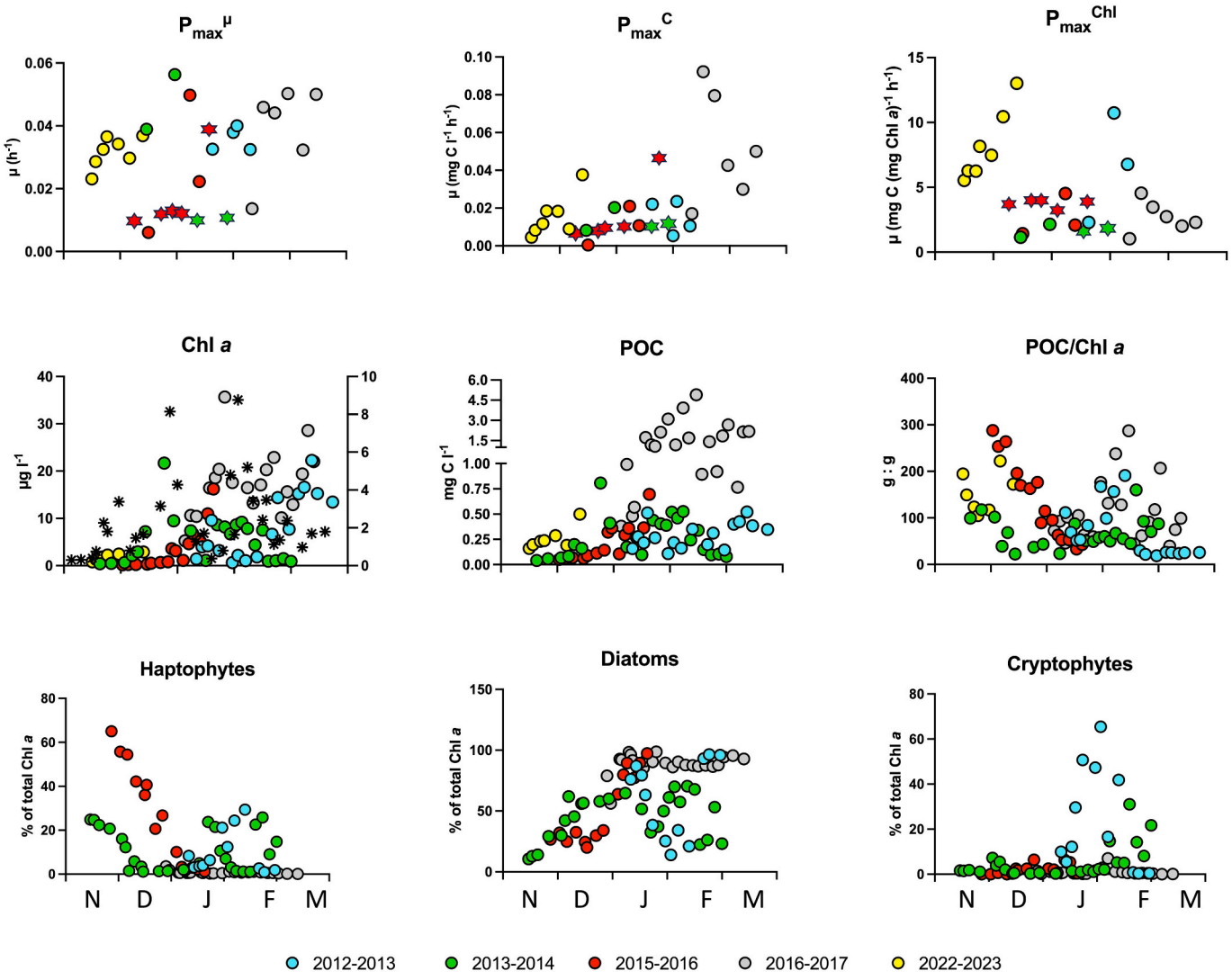

Fig. 3. Biological parameters from discrete samples taken at 15 m depth in Ryder Bay, recorded during the various surveys, between November (N) and March (M). Units: P^{μ}_{max} (h^{-1}); P^{C}_{max} (mg C l^{-1} h^{-1}); P^{Chl}_{max} (mg C (mg Chl *a*)$^{-1}$ h^{-1}); Chl *a* (μg l^{-1}); POC (mg C l^{-1}); POC/Chl a (g:g); haptophytes (%); diatoms (%); cryptophytes (%). Monthly averages of the dataset are given in Table 1. Note: Chl *a* in 2022–2023 was also plotted as derived from CTD-data (*; right axis). In 2013–2014 and 2015–2016, 15 m values were taken from the depth profiles (see Fig. 4); plotted as stars. Algal groups were only determined over the seasons of 2012–2013, 2013–2014, 2015–2016 and 2017. DOI: https://dataverse.nl/privateurl.xhtml?token=607fd7e1-77c8-4b48-9772-e669068dd9ad

with POC (Fig. 5, season, POC). The early season was correlated with presence of haptophytes, associated with lower temperatures (Fig. 5). The positive relationship between haptophytes and density (Fig. 5, Haptos, Dens) reflected more saline waters, compared to lower densities later in the season due to ongoing ice melt and fresh water-induced stratification. The presence of cryptophytes at the height of summer

(mainly in 2013, see Fig. 3) was positively correlated with high POC and production rates.

In 2022, microphytobenthos was extremely high in biomass and seen as fluff of algal material sometimes decreasing visibility as experienced by the Rothera scuba diving team. The benthic community was dominated by *Biddulphia* sp. and *Nitzschia* sp. (Bacillariophyceae). Specific growth rates (P^{μ}_{max} (h^{-1})) for the benthic community were two times lower than P^{μ}_{max} recorded for the pelagic community. Microphytobenthos also had a slightly lower photosynthetic yield (Table 1; *t*-test).

In 2014 and 2015–2016, algal production was recorded at various depths, at near optimal light conditions of 70 μmol photons m^{-2} s^{-1}; close to the E_k (Table 1). $P^{\mu}_{70\mu E}$ and $P^{C}_{70\mu E}$ increased over the course of summer (Fig. 4), with the highest rates recorded at 5 m in January 2016. $P^{Chl}_{70\mu E}$ was low in 2014, with hardly any changes in the water column and over time (Fig. 4). In 2015–2016, $P_{70\mu E}{}^{Chl}$ was more variable. In parallel, $P_{70\mu E}{}^{C}$ integrated over the top 40 m of the water column ($\sum PP$) also increased (Table 2). A high maximum value of circa 22 g C m^{-2} d^{-1} was recorded in January 2016.

3.2. Specific algal growth rates

In addition to the field study, specific growth rates of characteristic Antarctic phytoplankton species were retrieved from laboratory and literature studies (Table 3). Besides the ubiquitous haptophyte species *Phaeocystis antarctica* and *Chrysochromulina* sp., omnipresent diatom species were *Fragilariopsis* sp., *Nitzschia* sp., *Pseudo-nitzschia* sp., *Chaetoceros* sp. and *Thalassiosira* sp. These species were all observed in all seasons studied at Ryder Bay (see Table 3 in Van Leeuwe et al., 2020). The highest specific growth rates were recorded for diatoms as a group. Haptophytes had significantly lower growth rates (t-test, $p < 0.05$). The specific growth rates recorded in Ryder Bay were in the same order of magnitude as the rates recorded for the specific algal species. The differences between the various algal species were not significant. Only *Pseudo-nitzschia* sp. and *Chaetoceros* sp. had significantly higher growth rates (Table 3, t-test, $p < 0.05$).

Based on extensive literature- and laboratory studies, Coello-Camba and colleagues (2017) produced growth optima for a number of species (Table 3). The optimal temperatures for most species ranged between 2 and 5 degrees. The various diatoms had relatively high temperature growth optima, with an exceptionally high maximum of 7 °C recorded for *Chaetoceros* sp. (Table 3). The lowest temperature optimum was observed for the haptophyte *P. antarctica*.

4. Discussion

4.1. Primary production in Ryder Bay

Ryder Bay is a very productive area. High primary production rates support the biological carbon pump and the rich Antarctic food web (Clarke et al., 2007). Production rates of 0.010–0.040 mg C l^{-1} h^{-1} compare well with previous recordings in Ryder Bay (Rozema et al., 2017; Weston et al., 2013) and primary production in other polar coastal areas (Goldman et al., 2015; Mascioni et al., 2021; Moline et al., 1998). The depth-integrated production calculated in 2015–2016 of 410–2590 mg C m^{-2} d^{-1} is high compared to 100–1000 mg C m^{-2} d^{-1} recorded for coastal areas in Antarctica (Arrigo et al., 2015; Henley et al., 2019; Vernet et al., 2008), highlighting the biological importance of Ryder Bay.

Especially the high sea-ice years are associated with high phytoplankton biomass in the following summer season (Schofield et al., 2024; Venables et al., 2013). This was well illustrated in two out of the five seasonal studies. The studies in 2015–2016 and 2016–2017 concerned high-ice years, with prolonged sea-ice cover over winter (see Van Leeuwe et al., 2020). In 2016–2017, Ryder Bay had remained ice-covered until January 2017, followed by an immediate retreat of 2–3 days (Fig. 2). Algal growth increased rapidly after ice break-up. Stimulated by relatively calm summer conditions and very high production rates close to 0.1 mg C l^{-1} h^{-1}, a large algal bloom could develop (Fig. 3). Similar conditions explain the exceptionally high build-up of biomass in January 2016. Within 1–2 weeks after sea-ice retreat, primary production rates increased tenfold (Fig. 4), most likely supported by stratified waters that maintained algal communities high in the euphotic zone (Venable et al., 2013). Integrated primary production of more than 20 mg C m^{-2} d^{-1} were recorded (Table 2). These high production rates are out of range compared to average summer production rates, and are snapshots in time. Yet, they clearly illustrate the strong influence of sea-ice conditions on subsequent pelagic production, and explain the biological richness of the coastal areas of the WAP.

4.2. Specific production rates

In this study, primary production rates (P^{C}_{max}) were derived from specific production rates (P^{μ}_{max}). Whereas P^{C}_{max} is mostly relevant for carbon fluxes, P^{μ}_{max} provides more insight in the physiological capacity of the algal species involved. P^{C}_{max} was calculated by multiplying P^{μ}_{max} with the carbon concentration of the seawater, and is thereby influenced

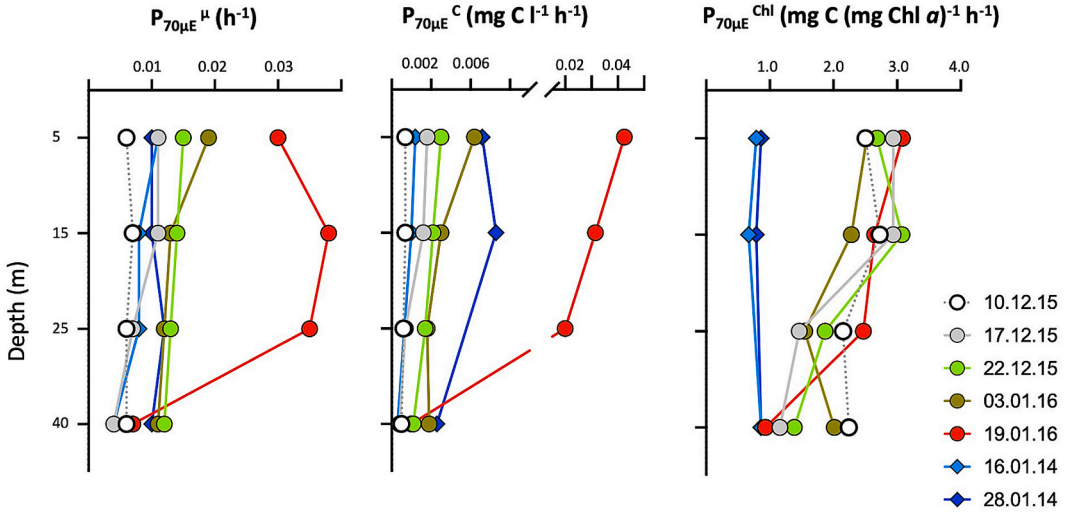

Fig. 4. Depth profiles of algal production rates in December 2015 and January 2016 (circles) and January 2014 (diamonds), expressed as $P^{\mu}_{70\mu E}$ (h^{-1}), $P^{C}_{70\mu E}$ (mg C l^{-1} h^{-1}) and $P^{Chl}_{70\mu E}$ (mg C (mg Chl *a*)$^{-1}$ h^{-1}).

Table 2
Depth integrated primary production $\sum PP$ (g C m^{-2} d^{-1}), calculated per day. Profiles were recorded in December–January 2015–2016 and in January 2014.

Date	10.12.15	17.12.15	22.12.15	03.01.16	19.01.16	16.01.14	28.01.14
$\sum PP$	0.41	0.81	1.43	1.91	22.19	0.55	2.59

Table 3
Average growth rates (d^{-1}) for algal species as derived from laboratory studies at the RUG, and literature (see Table S2). In addition, specific production rates (P^{μ}_{max}) were calculated per day for the in situ algal community in Ryder Bay.

	Species	μ (d^{-1})	Temp. optimum (°C)*
RUG	*P. antarctica* (Hapto)	0.32 ± 0.13	–
	Chrysochromulina (Hapto)	0.23 ± 0.13	–
	C. brevis (Bacil)	0.46 ± 0.02	–
	F. cylindrus (Bacil)	0.29 ± 0.14	–
Literature	*P. antarctica* (Hapto)	0.37 ± 0.11	2
	Corethron sp. (Bacil)	0.33 ± 0.13	4
	Nitzschia sp. (Bacil)	0.45 ± 0.11	4**
	Pseudo-nitzschia sp. (Bacil) [a]	0.56 ± 0.19	4
	F. cylindrus (Bacil)	0.41 ± 0.21	5
	Thalassiosira sp. (Bacil)	0.43 ± 0.12	5
	Chaetoceros sp. (Bacil)[a]	0.51 ± 0.16	7
Ryder Bay	In situ algal community***	0.47 (± 0.13)	–

The data taken from literature studies are arranged according to the temperature optima. The average of all 15 m ocean samples over 2012–2022 (P^{μ}_{max} (d^{-1})) is included for comparison ($n = 22$).
[a] Significantly higher growth rates (t-test).
* Data from Coello-Camba et al., 2017.
** Data from Edwards et al., 2016; Fiala and Oriol, 1990; Jacques, 1983
*** Based on P^{μ}_{max} (h^{-1}), assuming 16 productive hours in a day. Abbreviations: F: *Fragilariopsis*; Hapto: Haptophyceae; Bacil: Bacillariophyceae.

by loss factors such as grazing and viral lyses (Rozema et al., 2017). P^{μ}_{max}, on the other hand, reflects the capacity of carbon fixation per unit carbon biomass, and is a more direct measure of growth efficiency. Specific production rates were variable throughout the growth season, with no significant trend (Fig. 3).

The absence of any trend in P^{μ}_{max} (Fig. 3) suggested that growth conditions were nearly optimal in Ryder Bay. This observation was supported by the fact that the average in situ P^{μ}_{max} was not significantly lower compared to laboratory studies (Table 3). The spread in the data can potentially be explained by variations in environmental conditions during sampling events, with associated natural variations in algal biomass and fitness. In Ryder, the fairly constant values for P^{μ}_{max} are maintained by a seasonal succession in algal species. In spring, growth was triggered by increasing daylight, as illustrated by a high P^{Chl}_{max} and high growth efficiency α recorded in 2022 (Table 1). The high α values, ranging between 0.06 and 0.09 mg C (mg Chl *a*)$^{-1}$ h^{-1} (μmol photons m^{-2} s^{-1})$^{-1}$), are close to those what theoretically can be maximally achieved in photosynthesis, considering the minimum number of photons that is required for carbon fixation (Sakshaug and Slagstad, 1991). These photophysiological characteristics allow the ambient algal community to benefit optimally from the return of the sun.

The spring algal communities were dominated by haptophyte species like *Phaeocystis antarctica*. *P. antarctica* can make a head start when sea-ice has been present, as the ice forms a seeding source for pelagic growth (Van Leeuwe et al., 2022). When released in the seawater, *P. antarctica* can outcompete other species, not only due to its high light affinity (Goffart et al., 2000; Kropuenske et al., 2010), but also to its low temperature tolerance (Nissen and Vogt, 2021). The literature study on specific growth rates showed that *P. antarctica* had a much lower temperature optimum of 2 °C for growth compared to diatoms. Likewise, an extensive ecological niche study linking ocean phytoplankton species to specific temperature niches confirmed that *P. antarctica* (together with *P. pouchetii*) had the lowest temperature niche center of all species studied (Brun et al., 2015). The significance of temperature as a growth controlling factor was confirmed by Spearman Rank Correlation analyses. Rank correlation showed a negative relationship between haptophytes (including *P. antarctica*) and temperature (Fig. 5) in Ryder Bay, corroborating the findings on the species-specific temperature preferences (Table 3).

Later in the season, algal growth benefits from increased stratification of the water column. The depth profiles recorded in 2015–2016 show very well the increase in production rates over the season (Fig. 4). The positive correlation between P^{μ}_{max} and higher temperatures and lower seawater density (Fig. 5) confirmed the relationship between stratification and algal production. Under optimal growth conditions, algal growth can result in bloom formation. In Ryder Bay, the summer blooms are mostly dominated by centric diatoms, like *Chaetoceros* sp. (Annett et al., 2010; Van Leeuwe et al., 2020). The dominance of the species can be explained by their high specific growth rates combined with a high temperature optimum (Table 3). The fact that P^{μ}_{max} did not show any seasonal trend within and between seasons confirmed the successful adaptation of algal communities to the seasonal changes in environmental conditions.

In response to the seasonal decline in irradiance, algal cells naturally increase their chlorophyll *a* content, which would result in low POC/Chl a ratio's. This relationship was not established. In contrast, during the studies in spring 2013–2014 and 2015–2016, POC/Chl a in fact decreased (Fig. 3). This decline may be related to the decline in haptophytes, including *Phaeocystis antarctica*. In colonial form, this species produces mucus with a high carbon content (Schoemann et al., 2005). Likewise, the differences in the profiles of P^{Chl}_{max}, recorded in 2014 and 2015–2016 (Fig. 4), can possibly be explained by annual differences in light levels, in combination with differences in algal species composition.

Our field study in concurrence with Table 3 indicates that overall smaller centric diatom species are most resilient at higher temperatures, which gives them advantage in warmer surface waters (Antoni et al., 2024). However, it must be noted that the growth optima presented in Table 3 should be interpreted with care. Many studies have addressed the interaction of several parameters that influence growth rates, of which temperature is only one. As such, the growth rates presented provide mainly physiological support for their dominance in the field, rather than direct evidence for species dominance. In an elaborate study at the northern WAP, not centric, but pennate diatoms became more prominent during summer (Costa et al., 2023). A multitude of factors, including stratification, were discussed as driving factors. Clearly, temperature may set the first boundaries on algal growth rates, but interactive factors are no less important.

4.3. Benthic production

Primary production by microphytobenthic communities still represents a great unknown. Relatively few data are available on benthic systems in the Southern Ocean, with the exception of studies performed at King George Island (see e.g. Longhi et al., 2003; Prelle et al., 2022; Wulff et al., 2008). At Rothera Station, a marine team is present throughout the year. The team has been active for over two decades. According to their observations, at times benthic algal biomass can be extremely high in Ryder Bay, observed as fluffs on the ocean floor. However, the phytobenthos has never been studied. In 2022, biomass was again very high. This time, we decided to include benthic production in our survey. Benthic communities can hardly thrive under conditions with sea ice, as sea-ice with snow cover absorbs almost 99% of incident irradiance (Arndt et al., 2017). In 2022, the spring had been

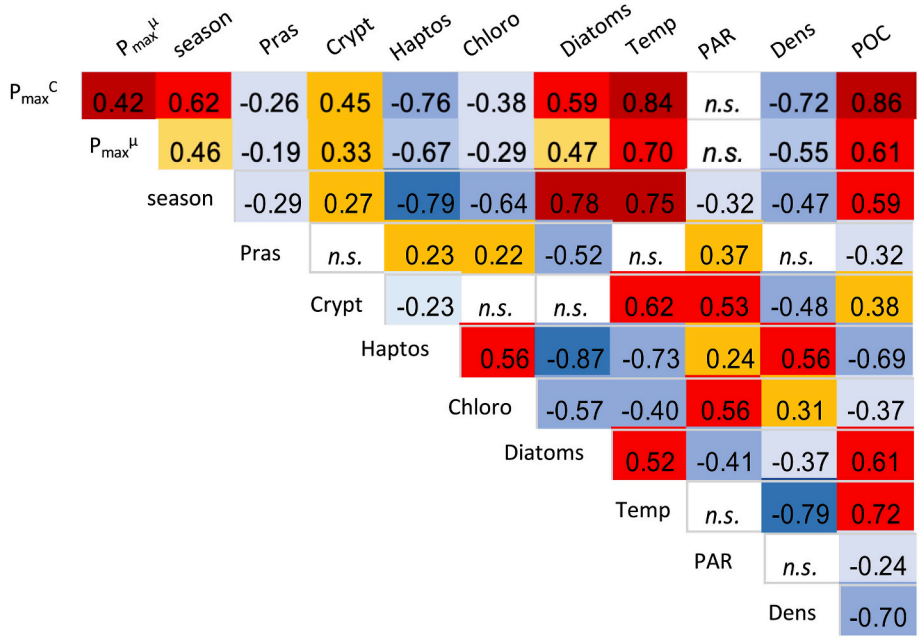

Fig. 5. Spearman Rank correlations between production rates and biological and oceanographic variables, for all data collected at the top 40 m, between 2012 and 2017. In warm colours significant positive correlations, in cold significant negative correlations. For abbreviations, see text.

without sea-ice cover, and it may be suggested that consequently more sunlight could reach the sea floor, to the benefit of benthic communities. The recorded specific production rates of the benthic community were significantly lower than the rates measured for pelagic communities (Table 1). However, literature indicates that benthic species (like various *Navicula* species) may reach growth rates up to 0.8 d^{-1} (Prelle et al., 2022), which is quite similar to pelagic species such as those shown in Table 3. Possibly, in Ryder Bay the benthic communities were nearing a state of senescence, though the photosynthetic yield was still relatively high. It must be noted that due to the sampling method applied, bias may have been introduced. The suction process disrupted the chain, which may have affected photophysiological responses. Although the specific benthic production rates of 0.018 h^{-1} were circa half of the rates recorded for the pelagic in 2022, it adds up to the pelagic production in feeding the marine system. Unfortunately, only one year of data was available, yet our findings do indicate that this as an area worthy of further study.

4.4. A changing ocean

Due to global warming, the marine ecosystem of the WAP is changing, with uncertainty surrounding the speed and direction that this change will take. Whereas it initially appeared that sea ice retreat resulted in a decline in algal biomass in the northern provinces of the WAP (Montes-Hugo et al., 2009), recent reviews showed an overall increase in primary production (Ferreira et al., 2024; Prakash et al., 2025; Schofield et al., 2024; Turner et al., 2024). This increase was associated with a later start of summer algal blooms, possible due to delayed stratification, albeit with a longer persistence. These developments could not yet be confirmed in Ryder Bay. In this more southern part of the Peninsula, oceanographic conditions in spring were still strongly governed by the dark and cold polar winter. Up to 2017, algal spring blooms were observed, associated with haptophytes species with a low temperature optimum. Sea ice had been absent in the spring of 2022, possibly marking the growing impact of climate change.

Along the full extent of the WAP, summer blooms will become increasingly more influenced by climate change and associated ocean warming. Initially, primary production rates are predicted to increase, based on the positive relationship between algal metabolic rates and seawater temperature (Davison, 1991). Dense algal blooms will be supported by more favorable oceanographic conditions (Garcia-Eidell et al., 2021). The potential impact of summer heatwaves is still hard to predict, but they will have a negative effect on primary production on a local scale (Latorre et al., 2023). Overall, current surface ocean temperatures of 1–2 °C (Antoni et al., 2024; Venables et al., 2023) are still far from the temperature optimum of the diatom communities that now thrive in Ryder Bay (Coello-Camba and Agustí, 2017; Edwards et al., 2016). However, it is quite likely that temperatures will exceed the upper limit for algal growth of the resident communities, already in the coming decades (e.g. Fiala and Oriol, 1990).

In Ryder Bay, shifts in species composition can be expected, alike the changes described in the northern WAP. Besides the intrusion of sub-Antarctic species like the diatom *Shionodiscus gaarderae* (Antoni et al., 2024), the algal community is likely to experience a more general shift towards the smaller size classes (Daufresne et al., 2009; Finkel et al., 2010). In Ryder Bay, the occasional blooms of cryptophytes as observed in 2013 and 2014, may be considered the first sentinel of shifting algal communities due to climate change as already observed in the northern WAP (Mendes et al., 2023). Yet, in the coming years, it seems reasonable to assume that the southern WAP will continue as a productive area.

5. Future perspectives

By the end of the century, ongoing warming may result in the rise of temperatures in surface waters by more than 3 °C in summer. At the same time, sea-ice extent could well have declined to a dramatic low extent (Kwiatkowski et al., 2020), which will negatively impact on the stability of the surface ocean. The algal landscape may then severely change. With the loss of sea-ice as a seeding source, and the potentially fatal effects of warming seawater, haptophyte species like *P. antarctica* will be under threat of becoming diminished (Xu et al., 2014; Zhu et al., 2016). Many polar diatom species might also vanish (Boyd et al., 2013) and subpolar species will likely continue to increase in numbers (Thomas et al., 2012). These shifts may come relatively rapidly, considering that temperature-growth relationships are not unimodal, but left-skewed to the lower temperatures; that is with a sharp drop in growth rates once a temperature threshold is exceeded (Eppley, 1972).

Moreover, temperature is just one of several drivers that are subject to climate change, such as nutrient- and light conditions and grazing pressure (Deppeler and Davidson, 2017). The multitude of interacting factors makes the future hard to predict, but abrupt changes in species composition with ongoing warming of surface waters can be foreseen.

Ultimately, the consequences for the marine ecosystem will be profound. A shift in species composition will impact on the marine foodweb, carbon fluxes and the role of the Southern Ocean in climate regulation (Clarke et al., 2007). Diatoms contribute strongly to primary production and are a significant food source for higher trophic levels (Schofield et al., 2024). In addition, the sequestration of atmospheric CO_2 by large diatom blooms may buffer anthropogenic CO_2-emissions. Haptophytes, including species such as *Phaeocystis antarctica* (Van Leeuwe et al., 2020) are not only associated with strong carbon fluxes into the deep ocean (DiTullio et al., 2000), but they can also play an alternative role in climate control through the production of the osmolyte dimethylsulfoniopropionate, which is the precursor of the climate active gas dimethylsulfide (DMS)(Stefels et al., 2007, 2018). Currently, Ryder Bay is a biological hotspot and a large sink for CO_2 (Droste et al., 2025), as well as an important source of DMS (Webb et al., 2019) and other climate regulating gases. All these ecosystem functions will decline, at a yet unknown pace.

CRediT authorship contribution statement

Maria A. van Leeuwe: Writing – original draft, Methodology, Investigation, Formal analysis, Conceptualization. **Alison L. Webb:** Writing – original draft, Methodology, Investigation, Formal analysis, Conceptualization. **Mareike G. Bach:** Writing – original draft, Methodology, Investigation, Formal analysis, Conceptualization. **Michael P. Meredith:** Writing – original draft, Methodology, Investigation, Formal analysis, Conceptualization. **Desiree den Os:** Writing – original draft, Methodology, Investigation, Formal analysis, Conceptualization. **Jacqueline Stefels:** Writing – original draft, Methodology, Investigation, Formal analysis, Conceptualization.

Funding

This work was supported by the Netherlands Organisation for Scientific Research (NWO) under the Polar Program (NPP) Project Numbers 866.10.101, 866.14.101 and ALWPP.2016.036. RaTS is a component of the BAS Polar Oceans research program, funded by the U. K. Natural Environment Research Council (NERC). The participation of MM was supported by NERC awards NE/Y006178/1 (PRESCIENT) and NE/W004933/1 (BIOPOLE).

Declaration of competing interest

The authors declare that they have no known competing financial interests or personal relationships that could influence the work reported in this paper.

Acknowledgements

We thank the marine technical staff at the British Antarctic Survey's Rothera Research Station for all general support. We are grateful to Nadia Frontier and Ryan Mathews for their support in 2022.

Appendix A. Supplementary data

Supplementary data to this article can be found online at https://doi.org/10.1016/j.jmarsys.2026.104271.

Data availability

Data will be made available on request.

References

Annett, A.L., Carson, D.S., Crosta, X., Clarke, A., Ganeshram, R.S., 2010. Seasonal progression of diatom assemblages in surface waters of Ryder Bay, Antarctica. Polar Biol. 33, 13–29. https://doi.org/10.1007/s00300-009-0681-7.

Antoni, J.S., Almandoz, G.O., Goldsmit, J., Garcia, M.D., Flores-Melo, X., Hernando, M. P., Schloss, I.R., 2024. Long-term studies on West Antarctic peninsula phytoplankton blooms suggest range shifts between temperate and polar species. Glob. Change Biol. 30, e17238. https://doi.org/10.1111/gcb.17238.

Arndt, S., Meiners, K.M., Ricker, R., Krumpen, T., Katlein, C., Nicolaus, M., 2017. Influence of snow depth and surface flooding on light transmission through Antarctic pack ice. J. Geophys. Res. Oceans 122, 2108–2119. https://doi.org/10.1002/2016JC012325.

Arrigo, K.R., van Dijken, G.L., Strong, A.L., 2015. Environmental controls of marine productivity hot spots around Antarctica. J. Geophys. Res. Oceans. 120, 5545–5565. https://doi.org/10.1002/2015JC010888.

Bown, J., Van Haren, H., Meredith, M.P., Venables, H.J., Laan, P., Brearley, J.A., De Baar, H.J.W., 2018. Evidence of strong sources of DFe and DMn in Ryder Bay, Western Antarctic peninsula. Philos. Trans. R. Soc. A Math. Phys. Eng. Sci. 376. https://doi.org/10.1098/rsta.2017.0172.

Boyd, P.W., Rynearson, T.A., Armstrong, E.A., Fu, F., Hayashi, K., Hu, Z., et al., 2013. Marine phytoplankton temperature versus growth responses from polar to tropical waters – outcome of a scientific community-wide study. PloS One 8 (5), e63091. https://doi.org/10.1371/journal.pone.0063091.

Boyd, P.W., Arrigo, K.R., Ardyna, M., Halfter, S., Huckstadt, L., Kuhn, A.M., et al., 2024. The role of biota in the Southern Ocean carbon cycle. Nat. Rev. Earth Environ. https://doi.org/10.1038/s43017-024-00531-3.

Brun, P., Vogt, M., Payne, M.R., Gruber, N., O'Brien, C.J., Buitenhuis, E.T., et al., 2015. Ecological niches of open ocean phytoplankton taxa. Limnol. Oceanogr. 60, 1020–1038. https://doi.org/10.1002/lno.10074.

Clarke, A., Murphy, E.J., Meredith, M.P., King, J.C., Peck, L.S., Barnes, D.K.A., Smith, R. C., 2007. Climate change and the marine ecosystem of the western Antarctic peninsula. Phil. Trans. Royal Soc. B 362, 149–166. https://doi.org/10.1098/rstb.2006.1958.

Clarke, A., Meredith, M.P., Wallace, M.I., Brandon, M.A., Thomas, D.N., 2008. Seasonal and interannual variability in temperature, chlorophyll and macronutrients in northern Marguerite Bay, Antarctica. Deep Sea Res. Part II: Topical Stud. Oceanogr. 55, 1988–2006. https://doi.org/10.1016/j.dsr2.2008.04.035.

Coello-Camba, A., Agustí, S., 2017. Thermal thresholds of phytoplankton growth in polar waters and their consequences for a warming Polar Ocean. Front. Mar. Sc. 4, 168. https://doi.org/10.3389/fmars.2017.00168.

Costa, R.R., Ferreira, A., de Souza, M.S., Tavano, V.M., Kerr, R., Secchi, E.R., Brotas, V., Dotto, T.S., Brito, A.C., Mendes, C.R.B., 2023. Physical-biological drivers modulating phytoplankton seasonal succession along the northern Antarctic peninsula. Environ. Res. 231, 116273. https://doi.org/10.1016/j.envres.2023.116273.

Daufresne, M., Lengfellner, K., Sommer, U., 2009. Global warming benefits the small in aquatic ecosystems. Proc. Natl. Acad. Sci. U. S. A. 106 (31), 12788–12793. https://Doi.org. https://doi.org/10.1073/pnas.0902080106.

Davison, I., 1991. Environmental effects on algal photosynthesis: temperature. J. Phycol. 27, 2–8. https://doi.org/10.1111/j.0022-3646.1991.00002.x.

Deppeler, S.I., Davidson, A.T., 2017. Southern Ocean phytoplankton in a changing climate. Front. Mar. Sc. 4, 40. https://doi.org/10.3389/fmars.2017.00040.

DiTullio, G., Grebmeier, J., Arrigo, K., Lizotte, M.P., Robinson, D.H., Leventer, A., et al., 2000. Rapid and early export of *Phaeocystis antarctica* blooms in the Ross Sea, Antarctica. Nature 404, 595–598. https://doi.org/10.1038/35007061.

Droste, E.S., Bakker, D.C.E., Venables, H.J., Jones, E.M., Meredith, M.P., Dall'Olmo, G., et al., 2025. Sea ice controls net ocean uptake of carbon dioxide by regulating wintertime stratification. Commun. Earth Environ. 6, 457. https://doi.org/10.1038/s43247-025-02395-x.

Ducklow, H.W., Clarke, A., Dickhut, R., Doney, S.C., Geisz, H., Huang, K., et al., 2012. The Marine System of the Western Antarctic Peninsula. In: Rogers, A.D., Johnston, N. M., Murphy, E.J., Clarke, A. (Eds.), Antarctic Ecosystems: An Extreme Environment in a Changing World, pp. 121–159.

Eayrs, C., Li, X., Raphael, M.N., Holland, D.M., 2021. Rapid decline in Antarctic Sea-ice in recent years hints at future change. Nature Geo. 14, 460–464. https://doi.org/10.1038/s41561-021-00768-3.

Edwards, K.F., Thomas, M.K., Klausmeier, C.A., Litchman, E., 2016. Phytoplankton growth and the interaction of light and temperature: A synthesis at the species and community level. Limnol. Oceanogr. 61, 1232–1244. https://doi.org/10.1002/lno.10282.

Eppley, R.W., 1972. Temperature and phytoplankton growth in the sea. Fish. Bull. 70, 1063–1085.

Eveleth, R., Cassar, N., Sherrell, R.M., Ducklow, H., Meredith, M.P., Venables, H.J., 2017. Ice melt influence on summertime net community production along the Western Antarctic peninsula. Deep Sea Res. II. 139, 89–102. https://doi.org/10.1016/j.dsr2.2016.07.016.

Ferreira, A., Mendes, C.R.B., Costa, R.R., Brotas, V., Tavano, V.M., Guerreiro, C.V., et al., 2024. Climate change is associated with higher phytoplankton biomass and longer blooms in the West Antarctic peninsula. Nat. Commun. 15, 6536. https://doi.org/10.1038/s41467-024-50381-2.

Fiala, M., Oriol, L., 1990. Light-temperature interactions on the growth of Antarctic diatoms. Polar Biol. 10 (8), 629–636. https://doi.org/10.1007/BF00239374.

Finkel, Z.V., Beardall, J., Flynn, K.J., Quigg, A., Rees, T.A.V., Raven, J.A., 2010. Phytoplankton in a changing world: cell size and elemental stoichiometry. J. Plankton Res. 32, 119–137.

Garcia-Eidell, C., Comiso, J.C., Berkelhammer, M., 2021. Interrelationships of sea surface salinity, chlorophyll-a concentration, and sea surface temperature near the Antarctic ice edge. J. Climate 34, 6069–6086. https://doi.org/10.1175/JCLI-D-20-0716.1.

Goffart, A., Catalano, G., Hecq, J.H., 2000. Factors controlling the distribution of diatoms and *Phaeocystis* in the Ross Sea. J. Mar. Syst. 27, 161–175.

Goldman, J.A.L., Kranz, S.A., Young, J.N., Tortell, P.D., Stanley, R.H.R., Bender, M.L., Morel, F.M.M., 2015. Gross and net production during the spring bloom along the Western Antarctic peninsula. New Phytol. 205, 182–191.

Henley, S.F., Schofield, O.M., Hendry, K.R., Schloss, I.R., Steinberg, D.K., Moffat, C., et al., 2019. Variability and change in the West Antarctic peninsula marine system: research priorities and opportunities. Progr. Oceanogr. 173, 208–237.

Henley, S.F., Ganeshram, R.S., Annett, A.L., Tuerena, R.E., Fallick, A.E., Meredith, M.P., et al., 2017. Macronutrient supply, uptake and recycling in the coastal ocean of the West Antarctic peninsula. Deep Sea Res. Part II Top. Stud. Oceanogr. 139, 58–76. https://doi.org/10.1016/j.dsr2.2016.10.003.

Höfer, J., Giesecke, R., Hopwood, M.J., Carrera, V., Alarcón, E., González, H.E., 2019. The role of water column stability and wind mixing in the production/export dynamics of two bays in the Western Antarctic peninsula. Progr. Oceanogr. 174, 105–116. https://doi.org/10.1016/j.pocean.2019.01.005.

Hughes, C., Chuck, A.L., Rossetti, H., Mann, P.J., Turner, S.M., Clarke, A., et al., 2009. Seasonal cycle of seawater bromoform and dibromomethane concentrations in a coastal bay on the western Antarctic peninsula. Glob. Biogeochem. Cycles 23, GB2024. https://doi.org/10.1029/2008GB003268.

Jacques, G., 1983. Some ecophysiological aspects of the Antarctic phytoplankton. Polar Biol. 2, 27–33.

Kropuenske, L.R., Mills, M.M., Van Dijken, G.L., Alderkamp, A.-C., Berg, G.M., Robinson, D.H., et al., 2010. Strategies and rates of photoacclimation in two major Southern Ocean phytoplankton taxa: *Phaeocystis antarctica* (haptophyta) and *Fragilariopsis cylindrus* (bacillariophyceae). J. Phycol. 46, 1138–1151.

van Leeuwe, M.A., Fenton, M., Davey, E., Rintala, J.M., Jones, E.M., Meredith, M.P., Stefels, J., 2022. On the phenology and seeding potential of sea-ice microalgal species. Elem. Sci. Anth. 10, 1. https://doi.org/10.1525/elementa.2021.00029.

Latorre, M.P., Iachetti, C.M., Schloss, I.R., Antoni, J., Malits, A., et al., 2023. Summer heatwaves affect coastal Antarctic plankton metabolism and community structure. J. Exp. Mar. Biol. Ecol. 567. https://doi.org/10.1016/j.jembe.2023.151926.

Longhi, M.L., Schloss, I.R., Wiencke, C., 2003. Effect of irradiance and temperature on photosynthesis and growth of two Antarctic benthic diatoms, *Gyrosigma subsalinum* and *Odontella litigiosa*. Bot. Mar. 46, 276–284.

Mascioni, M., Almandoz, G.O., Ekern, L., Pan, B.J., Vernet, M., 2021. Microplanktonic diatom assemblages dominated the primary production but not the biomass in an Antarctic fjord. J. Mar. Syst. 224. https://doi.org/10.1016/j.jmarsys.2021.103624.

Mendes, C.R.B., Costa, R.R., Ferreira, A., Jesus, B., Tavano, V.M., Dotto, T.S., et al., 2023. Cryptophytes: an emerging algal group in the rapidly changing Antarctic Peninsula marine environments. Glob. Change Biol. https://doi.org/10.1111/gcb.16602.

Meredith, M.P., King, J.C., 2005. Rapid climate change in the ocean west of the Antarctic peninsula during the second half of the 20th century. Geophys. Res. Lett. 32, 1–5. https://doi.org/10.1029/2005GL024042.

Moline, M.A., Schofield, O., Boucher, N.P., 1998. Photosynthetic parameters and empirical modelling of primary production: a case study on the Antarctic peninsula shelf. Ant. Sc. 10 (1), 45–54.

Moline, M.A., Claustre, H., Frazer, T.K., Schofield, O., Vernet, M., 2004. Alteration of the food web along the Antarctic peninsula in response to a regional warming trend. Glob. Change Biol. 10, 1973–1980. https://doi.org/10.1111/j.1365-2486.2004.00825.x.

Montes-Hugo, M., Doney, S.C., Ducklow, H.W., Fraser, W.R., Martinson, D., Stammerjohn, S.E., et al., 2009. Recent changes in phytoplankton communities associated with rapid regional climate change along the western Antarctic peninsula. Science 323, 1470–1473. https://doi.org/10.1126/science.1164533.

Moreau, S., Mostajir, B., Belanger, S., Schloss, I., Vancoppenolle, M., Demers, S., Ferreyra, G., 2015. Climate change enhances primary production in the western Antarctic peninsula. Glob. Change Biol. 21, 2191–2205.

Nissen, C., Vogt, M., 2021. Factors controlling the competition between *Phaeocystis* and diatoms in the Southern Ocean and implications for carbon fluxes. Biogeoscience 18, 251–283.

Platt, T.C., Gallegos, C.L., Harrison, W.G., 1980. Photoinhibition of photosynthesis in natural assemblages of marine phytoplankton. J. Mar. Res. 38, 687–701.

Prakash, P., Mohan, R., Naik, R.K., Luis, A.J., 2025. Phytoplankton dynamics in the Antarctic marginal ice zone: trends and drivers. J. Mar. Syst. 248, 104044. https://doi.org/10.1016/j.jmarsys.2025.104044.

Prelle, L.R., Schmidt, I., Schimani, K., Zimmermann, J., Abarca, N., Skibbe, O., et al., 2022. Photosynthetic, respirational, and growth responses of six benthic diatoms from the Antarctic peninsula as functions of salinity and temperature variations. Genes 13, 1264. https://doi.org/10.3390/genes13071264.

Reid, P., Stammerjohn, S., Massom, R.A., Barreira, S., Scambos, T., Lieser, J.L., 2020. Sea ice extent, concentration, and seasonality (in "state of the climate in 2019"). Bull. Am. Met. Soc. 101 (8), S304–S306. https://doi.org/10.1175/BAMS-D-20-0090.1.

Rozema, P.D., Kulk, G., Veldhuis, M.P., Buma, A.G.J., Meredith, M.P., Van de Poll, W.H., 2017. Assessing drivers of coastal primary production in northern Marguerite Bay, Antarctica. Front. Mar. Sci. 4, 184. https://doi.org/10.3389/fmars.2017.00184.

Sakshaug, E., Slagstad, D., 1991. Light and productivity of phytoplankton in polar marine ecosystems: a physiological view. Polar Res. 10, 69–85.

Schoemann, V., Becquevort, S., Stefels, J., Rousseau, V., Lancelot, C., 2005. *Phaeocystis* blooms in the global ocean and their controlling mechanisms: a review. J. Sea Res. 53, 43–66. https://doi.org/10.1016/j.seares.2004.01.008.

Schofield, O., Cimino, M., Doney, S., Friedlaender, A., Meredith, M.P., Moffat, C., et al., 2024. Antarctic pelagic ecosystems on a warming planet. Trends Ecol. Evol. 3345. https://doi.org/10.1016/j.tree.2024.08.007.

Smetacek, V., Scharek, R., Nothig, E.M., 1990. Seasonal and regional variation in the pelagial and its relationship to the life history cycle of krill. In: Kerry, K.R., Hempel, G. (Eds.), Antarctic Ecosystems. Ecological change and conservation. Springer-Verlag Berlin Heidelberg, pp. 103–113.

Smith, W.O., Comiso, J.C., 2008. The influence of sea ice on primary production in the Southern Ocean: a satellite perspective. J. Geophys. Res. 113, C05S93. https://doi.org/10.1029/2007JC004251.

Stammerjohn, S.E., Drinkwater, M.R., Smith, R.C., Liu, X., 2003. Ice-atmosphere interactions during sea-ice advance and retreat in the western Antarctic peninsula region. J. Geophys. Res. 108 (C10). https://doi.org/10.1029/2002JC001543.

Stammerjohn, S.E., Martinson, D.G., Smith, R.C., Iannuzzi, R.A., 2008. Sea ice in the western Antarctic peninsula region: Spatio-temporal variability from ecological and climate change perspectives. Deep-Sea Res. II 55, 2041–2058. https://doi.org/10.1016/j.dsr2.2008.04.026.

Stammerjohn, S.E., Eayrs, C., Haumann, F.A., Hobbs, W., Holland, M., Reid, P., Roach, L. A., Smith, S., 2025. Antarctic Sea-ice. Ongoing changes and compelling issues. In: Meredith, M.P., Melbourne-Thomas, J., Garabato, A.C.N., Raphael, M. (Eds.), Antarctica and the Earth System. Routlegde. https://doi.org/10.4324/9781003406471-6.

Stefels, J., Steinke, M., Turner, S., Malin, G., Belviso, S., 2007. Environmental constraints on the production and removal of the climatically active gas dimethyl-sulphide (DMS) and implications for ecosystem modelling. Biogeochem 83, 245–275. https://doi.org/10.1007/s10533-007-9091-5.

Stefels, J., Dacey, J.W.H., Elzenga, J.T.M., 2009. In vivo DMSP-biosynthesis measurements using stable-isotope incorporation and proton-transfer-reaction mass spectrometry (PTR-MS). Limnol. Oceanogr. Methods 7, 595–611.

Stefels, J., van Leeuwe, M.A., Jones, E.J., Meredith, M.P., Venables, H.J., Webb, A.L., Henley, S.F., 2018. Impact of sea-ice melt on DMS(P) inventories in surface waters of Marguerite Bay, West Antarctic peninsula. Phil. Trans. Royal Society A. 376, 20170169.

Thomas, M.K., Kremer, C.T., Klausmeier, C.A., Litchman, E., 2012. A global pattern of thermal adaptation in marine phytoplankton. Science 338, 1085–1088. https://doi.org/10.1126/science.1224836.

Turner, J.S., Dierssen, H., Schofield, O., Kim, H.H., Stammerjohn, S., Munro, D.R., Kavanaugh, M., 2024. Changing phytoplankton phenology in the marginal ice zone west of the Antarctic peninsula. Mar. Ecol. Prog. Ser. 734, 1–21. https://doi.org/10.3354/meps14567.

Van Leeuwe, M.A., Webb, A.L., Venables, H.J., Visser, R.J.W., Meredith, M.P., Elzenga, J. T.M., Stefels, J., 2020. Annual patterns in phytoplankton phenology in Antarctic coastal waters explained by environmental drivers. Limnol. Oceanogr. 1651–1668. https://doi.org/10.1002/lno.11477.

Venables, H.J., Clarke, A., Meredith, M.P., 2013. Wintertime controls on summer stratification and productivity at the western Antarctic peninsula. Limnol. Oceanogr. 58, 1035–1047. https://doi.org/10.4319/lo.2013.58.3.1035.

Venables, H.J., Meredith, M.P., Hendry, K.R., ten Hoopen, P., Peat, H., et al., 2023. Sustained year-round oceanographic measurements from Rothera Research Station, Antarctica, 1997-2017. Nature Sci. Data. 10, 265. https://doi.org/10.1038/s41597-023-02172-5.

Vernet, M., Martinson, D., Iannuzzi, R., Stammerjohn, S., Kozlowski, W., Sines, K., et al., 2008. Primary production within the sea-ice zone west of the Antarctic peninsula: I-sea ice, summer mixed layer, and irradiance. Deep Sea Res. Part II Top. Stud. Oceanogr. 55, 2068–2085. https://doi.org/10.1016/j.dsr2.2008.05.021.

Webb, A., Van Leeuwe, M.A., den Os, D., Meredith, M.P., Venables, V., Stefels, J., 2019. Extreme spikes in DMS flux double estimates of biogenic sulfur export from the Antarctic coastal zone to the atmosphere. Nat. Sci. Rep. 9, 2233. https://doi.org/10.1038/s41598-019-38714-.

Weston, K., others, 2013. Primary production export flux in Marguerite Bay (Antarctic peninsula): linking upper water-column production to sediment trap flux. Deep. Res. Part I Oceanogr. Res. Pap. 75, 52–66. https://doi.org/10.1016/j.dsr.2013.02.001.

Wulff, A., Roleda, M.Y., Zacher, K., Wiencke, C., 2008. Exposure to sudden light burst after prolonged darkness—A case study on benthic diatoms in Antarctica. Diatom Res. 23, 519–532.

Xu, K., Fu., F.-X., Hutchins, D.A., 2014. Comparative responses of two dominant Antarctic phytoplankton taxa to interactions between ocean acidification, warming, irradiance, and iron availability. Limnol. Oceanogr. 59 (6), 1919–1931.

Zhu, Z., Xu, K., Fu, F., Spackeen, J.L., Bronk, D.A., Hutchins, D.A., 2016. A comparative study of iron and temperature interactive effects on diatoms and *Phaeocystis antarctica* from the Ross Sea, Antarctica. Mar. Ecol. Prog. Ser. 550, 39–51.